# Hyperspectral two-photon excitation microscopy using visible wavelength

**TOSHIKI KUBO[1, 2], KENTA TEMMA[1, 2], NICHOLAS I. SMITH[3], KAI LU[4], TOMOKI MATSUDA[4], TAKEHARU NAGAI[4, 5], AND KATSUMASA FUJITA[1, 2, 5,*]**

[1]*Advanced Photonics and Biosensing Open Innovation Laboratory, AIST-Osaka University, Osaka University, Suita, Osaka 565-0871, Japan*
[2]*Department of Applied Physics, Osaka University, Suita, Osaka 565-0871, Japan.*
[3]*Immunology Frontier Research Center, Osaka University, Suita, Osaka 565-0871, Japan*
[4]*The Institute of Scientific and Industrial Research, Osaka University, Ibaraki, Osaka 567-0047, Japan*
[5]*Institute for Open and Transdisciplinary Research Initiatives, Osaka University, Suita, Osaka 565-0871, Japan*
**Corresponding author: fujita@ap.eng.osaka-u.ac.jp*

Received XX Month XXXX; revised XX Month, XXXX; accepted XX Month XXXX; posted XX Month XXXX (Doc. ID XXXXX); published XX Month XXXX

**We demonstrate hyperspectral imaging by visible-wavelength two-photon excitation microscopy using line illumination and slit-confocal detection. A femtosecond pulsed laser light at 530 nm was used for the simultaneous excitation of fluorescent proteins with different emission wavelengths. The use of line illumination enabled efficient detection of hyperspectral images and achieved simultaneous detection of three fluorescence spectra in the observation of living HeLa cells with an exposure time of 1 ms per line, which is equivalent to about 2 μs per pixel in point scanning, with 160 data points per spectrum. On combining linear spectral unmixing techniques, localization of fluorescent probes in the cells was achieved. A theoretical investigation of the imaging property revealed high-depth discrimination property attained through the combination of nonlinear excitation and slit detection.**


http://dx.doi.org/10.1364/OL.99.099999

Fluorescence microscopy is a powerful tool to investigate biological functions of intracellular molecules which involve the interactions between different proteins and other types of molecules. Fluorescent probes are typically used to specifically visualize the distributions and dynamics of intracellular molecules and monitor their interactions [1,2]. Multiple fluorescent probes with different emission wavelengths are typically used to observe the dynamics and interactions of different molecular species that result from complex biological events inside the cells [3].

One technique for imaging multicolor-stained samples is by detecting fluorescence with multiple spectral windows and unmixing their overlapping fluorescence emission. The additional use of multiple excitation wavelengths is also often necessary since the probes can have unique characteristic absorption and emission spectra. Multiple fluorescent proteins used for staining a sample then require an increased number of excitation light sources. High-speed switching of excitation and detection wavelengths [4] enables temporal separation of fluorescence emission; however, multiple probes are simultaneously detected.

Recently, the use of visible wavelengths for two-photon excitation in multicolor fluorescence imaging has been demonstrated [5,6]. It has also been discussed that a high-absorption two-photon cross section can be realized via pre-resonant two-photon excitation, which is observed when the excitation energy is slightly smaller than the band gap, in the visible-wavelength two-photon excitation (v2PE) of fluorescent proteins [7-9]. In our study, we have expanded the use of v2PE by utilizing the absorption band in the DUV region to induce fluorescence emission at the visible wavelength. Since many useful fluorescent proteins share absorption features in the DUV region (250–300 nm), single-wavelength pulsed irradiation of the wavelength range around 500–600 nm can excite multiple fluorescent proteins simultaneously via two-photon absorption. It also allows the fluorescence excitation from a wide range covering violet to red wavelengths using a single wavelength for both single- and two-photon excitation. In addition, the nonlinear excitation at a shorter wavelength provides higher spatial resolution than conventional one-photon excitation confocal microscopy.

In this letter, to expand the capability of v2PE for simultaneous multicolor imaging, we demonstrate hyperspectral v2PE imaging using slit-scanning confocal microscopy. The spectral detection is useful to distinguish small differences in the shape of the emission spectra, which provides us with more choices of fluorescent proteins for simultaneous multicolor imaging. As the spectra of fluorescent proteins have a similar peak wavelength with a broad shape, they tend to cause crosstalk with each other [10]. The crosstalk makes it difficult to divide the emission from different types of fluorescent proteins using glass filters [11]. In hyperspectral imaging, spectral information helps us to choose

wavelength regions for performing fluorescence unmixing and enables us to distinguish different fluorescent proteins.

We adopted slit-scanning confocal microscopy [12,13] in order to achieve hyperspectral imaging without affecting imaging speed. Generally, hyperspectral imaging requires relatively a long exposure time because the fluorescence signal is separated into multiple pixels on a one-dimensional (1D) or two-dimensional (2D) detector. In our microscope, a line-shaped excitation focus was used to detect fluorescence spectra from multiple probes simultaneously. This configuration has been used in NIR two-photon microscope [14] and Raman microscope [15] to perform hyperspectral imaging without affecting the temporal resolution significantly.

Fig. 1 shows the schematic of the optical setup constructed in this study. An NIR pulsed beam from a mode-locked Ti:Sapphire laser (Spectra physics, Mai tai HP) was converted into a visible-wavelength pulsed beam by an optical parametric oscillator (OPO) (Spectra-Physics, HF100) with a resulting pulse width and repetition rate of 200 fs and 80 MHz, respectively. The intensity profile of the laser beam was cleaned by a pinhole placed between a pair of relay lenses. A cylindrical lens was placed to form a line-shaped focus at the sample plane. A silicone-immersion objective lens (Olympus Corporation, UPlanSApo, ×60 NA 1.30 Sil) was used for the excitation and detection of fluorescence. Fluorescence emitted from the illuminated line on the sample was collected by the same objective lens and imaged on a slit with a width corresponding to 1 Airy unit (AU) at the central wavelength of detection. The fluorescence signal was separated from the excitation light by a combination of a short-pass filter (Semrock, FF01-533/SP-25) and a bandpass filter (Semrock, FF02-460/80). The 1D hyper spectral image was detected through a home-built imaging spectrophotometer using a prism (Thorlabs, PS855) and a sCMOS camera (Hamamatsu, Orca Flash 4.0 v3). A single-axis galvanometer mirror (GSI Lumonics, M2ST) was used to scan the laser focus in the direction perpendicular to the line illumination in order to perform 2D hyperspectral imaging.

To evaluate the capability of hyperspectral imaging of biological samples in our setup, we observed a living HeLa cell labeled with mseCFP [16], mTFP1 [17], and EGFP [18], localized at histone H2B, Golgi apparatus, and fibrillarin, respectively. Figs. 2(a)-(c) show the fluorescence images reconstructed by averaging fluorescence intensity in different regions of the detection wavelength. Fig. 2(d) depicts an image after the linear unmixing of the multicolor images

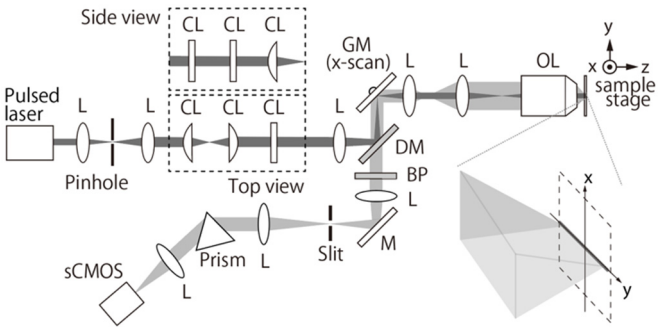


**Fig. 1.** Optical setup. L, CL, DM, GM, OL, M and BP represent the lens, cylindrical lens, dichroic mirror, galvanometer mirror, objective lens mirror, and bandpass filter, respectively.

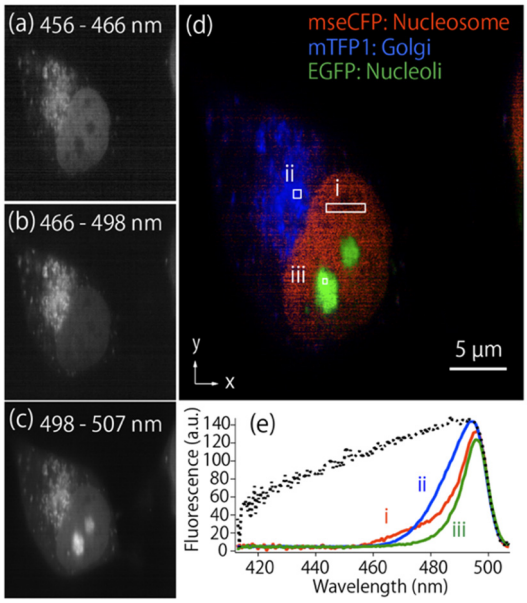


**Fig. 2.** Fluorescence images of a living HeLa cell expressing mseCFP, mTFP1, and EGFP at H2B, Golgi apparatus, and fibrillarin, respectively. (a)–(c) show the images constructed by fluorescence intensity in the spectral windows of 456–466 nm, 466–498 nm, and 498–507 nm, respectively. (d) shows the image reconstructed by spectral unmixing. (e) shows the fluorescence color spectra obtained by averaging the areas indicated by the squares in panel (d), along with the overall detection efficiency of the system shown by the dashed black line. The laser intensity and the length of the line focus were 270 kW/cm$^2$ and 30 μm at the focal plane of the objective lens, respectively.

in Figs. 2(a)-(c). The un-mixing was performed with reference spectra shown in Fig. 2(e), which are obtained by averaging the signal in the areas indicated by the squares (i)–(iii) in Fig. 2(d) [10]. We measured the detection efficiency of the system by measuring the spectrum of halogen lamp whose emission spectrum was known. The fluorescence signals are relatively low in the shorter-wavelength region because of the low sensitivity of the camera and the reflectivity of the mirrors used in the setup. The pixel number of the image was 610 and 700 in the horizontal (scanning) and vertical (line) directions, respectively. The number of data points in the spectral dimension was 160. The exposure time per line was 1 ms, which corresponds to about 2 μs per pixel in point scanning.

We also performed multicolor imaging of cells stained with four different fluorescent proteins using the same setup. We used living HeLa cells expressing Sirius [19], mseCFP, mTFP1, and EGFP at mitochondria, H2B, the Golgi, and fibrillarin, respectively. Fig. 3(a), (b), (c), and (d) show the images of average fluorescence intensity in different regions of the detection wavelength. Fig. 3(e) shows the multicolor image, which was constructed by merging the images shown in Figs. 3(a)–(d). No image processing was applied to these images. Fig.3(e) demonstrates that, even without the unmixing, a flexible choice of wavelength regions for image reconstruction enables us to visualize the cellular components with different colors. Fig. 3(f) shows that different types of fluorescent proteins can also be investigated with the spectra at local positions. The pixel number of the image is 1024 and 700 in the horizontal and vertical directions, corresponding to scanning and line directions, respectively. The data point in the spectral dimension was 160.

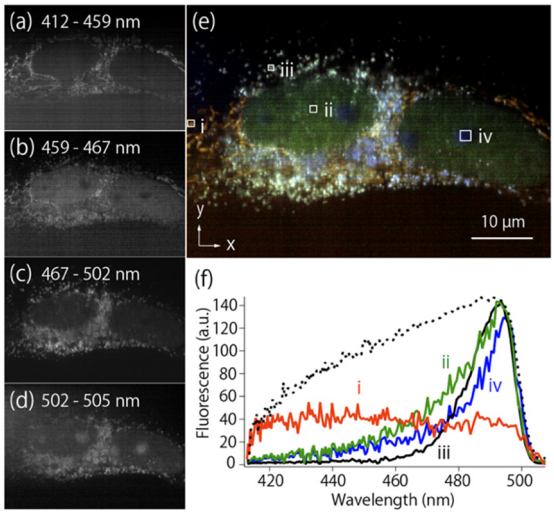


**Fig. 3.** Multicolor fluorescence image of a living HeLa cell expressing Sirius, mseCFP, mTFP1, and EGFP at mitochondria, histone H2B, the Golgi, and fibrillarin, respectively. (a) –(d) show the images constructed by averaging fluorescence intensity within the range of the detection wavelength from 410–459 nm, 459–467 nm, 467–502 nm, and 502–505 nm, respectively. (e) shows the reconstructed image given by merging (a)–(d). (f) shows the detection efficiency of the system by the dashed line curve, along with the measured spectra averaged from the areas indicated by squares in (e). The laser intensity and the length of the line focus were 270 kW/cm$^2$ and 30 μm, respectively, at the focal plane of the objective lens. The exposure time was 50 ms per line.

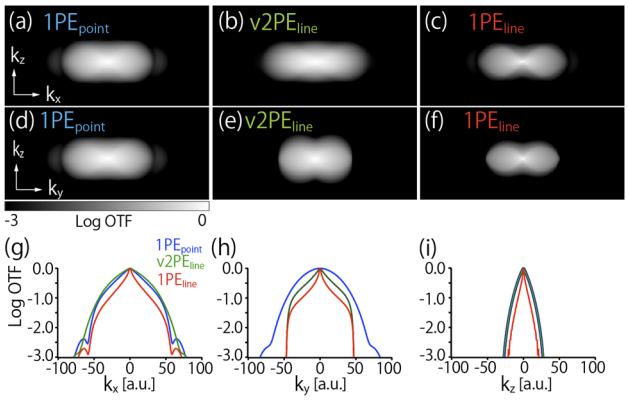


**Fig. 4.** The effective optical transfer functions (OTFs) of point-scanning 1PE ((a) and (d)), slit-scanning v2PE ((b) and (e)), and slit-scanning 1PE ((c) and (f)) microscopy. OTFs on the $k_x$-$k_z$ and $k_y$-$k_z$ planes are shown in (a)–(c) and (d)–(f), respectively. (g), (h), and (i) show the line profile of each OTF on the $k_x$, $k_y$, and $k_z$ axis, respectively.

While a slit-scanning confocal microscope realizes a temporal resolution higher than a point-scanning confocal microscope, the spatial resolution in the line and axial direction is compromised [20]. Although the lateral resolution in the direction parallel to the line illumination is the same as that obtained from wide-field fluorescence microscopy, the axial resolution can benefit from nonlinear two-photon excitation. As the slit cannot replace a spatial filter as effectively as the pinhole, the localization of two-photon excitation within the line-shaped focus is practically beneficial in the observation of samples containing 3D microstructures.

In order to evaluate the spatial resolution of v2PE microscopy with slit detection, we calculated the optical transfer functions (OTFs) of the systems using slit detection and one-photon excitation (1PE) as well as v2PE. We also calculated an OTF for a point-scanning system using a 1PE for comparison. The OTFs were calculated by determining the Fourier transform of the effective point spread functions after normalizing their peak intensities. Effective PSFs were calculated by the scalar Debye diffraction integral which takes the inclination factor into account [21]. Here, we assumed that the wavelengths of 1PE, v2PE, and fluorescence were 405 nm, 530 nm, and 440 nm, respectively, detected by a silicone-oil immersion objective lens with an NA of 1.3. The direction of laser scanning in the slit-scanning system was along the x-axis. The slit width and the pinhole diameter for point-scanning were set to 1 AU for the fluorescence wavelength. A smaller pinhole or slit can provide a stronger confocal effect resulting in higher resolution and sectioning capability. However, it is not practical to use a size smaller than 1 AU, especially in hyperspectral imaging, because it limits the signal-to-noise ratio significantly.

Figure 4 shows the calculated OTFs. The value is represented in the log scale. In the x-direction, which is perpendicular to the line illumination, the resolution of v2PE slit-scanning confocal microscopy is close to that of 1PE point- and slit-scanning confocal microscopy. In the y-direction, which is parallel to the line illumination, the resolution of v2PE slit-scanning confocal microscopy is the same as that of slit-scanning 1PE microscopy and lower than that of the point-scanning 1PE, because the principle of the image formation in slit-scanning confocal microscopy is wide-field imaging. In the z-direction, the resolution of v2PE slit-scanning confocal microscopy is higher than 1PE slit-scanning and almost the same as 1PE point-scanning confocal microscopy.

Although much shorter excitation wavelength was used in the calculation of the 1PE cases and a slit provides less sectioning than a pinhole, v2PE slit-scanning confocal microscopy provides similar resolution in the x and z direction with point-scanning 1PE confocal microscopy. Our method shows high resolution in the focusing direction and high depth discrimination by the combination of the 2nd-order nonlinearity of v2PE and slit detection.

In this paper, we demonstrated the use of v2PE in slit-scanning confocal microscopy to achieve hyperspectral imaging of fluorescent proteins by a single-wavelength excitation. We performed simultaneous multicolor fluorescence imaging of living HeLa cells by obtaining the fluorescence spectra of each type of fluorescent protein. The exercise enabled us to distinguish their distribution in the cells. We also performed the imaging using different combinations of fluorescent proteins without changing the detection system. Spectral detection has advantages over filter-based multicolor imaging in that there is no loss of fluorescence signal as it consists of using glass filter around the edge wavelength. Another advantage is that the detection system does not need to be redesigned when observing different fluorescent probe type samples, unlike filter-based imaging, where the set of filters needs to be changed according to the selected fluorophore.

In our system, it is also possible to increase the number of species, which can be detected by the fluorescence probes. However, to unmix multiple overlapping spectra, a high signal-to-noise ratio in spectral detection is required. In addition, by utilizing 1PE at the same wavelength for v2PE to excite yellow and red

fluorescent proteins [22,23], we can further increase the number of fluorescent probes for staining multiple targets.

Compared with the point-scanning v2PE confocal microscopy, the imaging speed of our line-illumination system is higher owing to the combination of the line illumination and parallel detection of fluorescence. The exposure time of the measurement is as low as 1 ms per line, which is comparable to the exposure time per pixel in point-scanning v2PE microscopy, resulting in an improvement of speed by two orders of magnitude. Under the same total imaging time, line-illumination offers a lower excitation intensity compared to single point-scanning, which is advantageous in avoiding photodamage nonlinearly proportional to the excitation intensity. Note that the photobleaching and photodamage in two-photon excitation shows a nonlinear response to excitation intensity higher than 2$^{nd}$ order [24, 25, 26]. Brief investigation of the photo-damage in hyper spectral v2PE imaging is given in Supplement 1.

One of the current limitations in our setup is the field of view (FOV). For imaging a larger FOV in our setup, using longer line illumination is effective if the laser power is sufficient for two-photon excitation over the illuminated area. In our setup, the maximum intensity obtained using the objective lens was 40 mW, which allows only an illumination length of 30 μm. One method to overcome this problem is by employing point focus illumination with fast scanning in one direction, which works similarly to line illumination [12,27,28]. However, this can increase the photodamage of samples because of the requirement of a high intensity excitation for a short pixel dwell time. Considering that the two-photon excitation at a shorter wavelength induces more photo-bleaching [9,29,30], the damage increase by the use of higher intensity should be more serious in v2PE than NIR two-photon excitation. Another method is the use of a lower repetition frequency of pulse light with a high peak power [31].

An advantage of our system compared with the simultaneous multicolor imaging by a confocal microscope using multiwavelength one-photon excitation is that it is not required to align the optics for overlapping multiple laser spots in a sample. The difference of the spot positions in a typical multiwavelength system results in the localization error. This chromatic aberration occurs as well as the inevitable chromatic aberrations in the detection side. In our system, since the excitation of all fluorophores is done by only one laser spot, chromatic aberrations are significantly reduced and occur only on the detection side.

The OTFs revealed the asymmetric spatial resolution in the x- and y-directions, which causes asymmetry of structures in the fluorescence image. This can be compensated by utilizing structured illumination to increase the resolution in y-direction [32,33], which is also useful to improve the axial resolution [34].

**Funding.** JST CREST (JPMJCR15N3); JSPS Grant-in-Aid for Scientific Research on Innovative Areas (18H05410).

**Acknowledgment**. A part of this work was performed under the Cooperative Research Program of the "Network Joint Research Center for Materials and Devices: Dynamic Alliance for Open Innovation Bridging Human, Environment and Materials" . Portions of this work were presented at the 6th Biomedical Imaging and Sensing Conference in 2020 (Proc. SPIE 11521,1152117).

**Disclosures**. The authors declare no conflicts of interest.

See Supplement 1 for supporting content.

## References

1. R. N. Day and M. W. Davidson, Chem. Soc. Rev. **38**, 2887 (2009).
2. J. Lippincott-Schwartz and G. H. Patterson, Science **300**, 87 (2003).
3. J. Ellenberg, J. Lippincott-Schwartz and J. F. Presley, Trends Cell Biol. **9**, 52 (1999).
4. Q. Li, X. He, Y. Wang, H. Liu, D. Xu and F. Guo, J. Biomed. Opt. **18**, 100901 (2013).
5. M. Yamanaka, K. Saito, N. I. Smith, Y. Arai, K. Uegaki, Y. Yonemaru, K. Mochizuki, S. Kawata, T. Nagai and K. Fujita, J. Biomed. Opt. **20**, 101202 (2015).
6. R. Oketani, H. Suda, K. Uegaki, T. Kubo, T. Matsuda, M. Yamanaka, Y. Arai, N. I. Smith, T. Nagai and K. Fujita, J. Biomed. Opt. **25**, 014502 (2019).
7. M.Drobizhev, F. Meng, A. Rebane, Y. Stepanenko, E. Nickel and C. W. Spangler, J. Phys. Chem. B **110**, 9802 (2006).
8. M. Drobizhev, N. S. Makarov, T. E. Hughes and A. Rebane, J. Phys. Chem. B **111**, 14051 (2007).
9. M. Drobizhev, N. S. Makarov, S. E. Tillo, T. E. Huges and A. Rebane, Nat. Methods **8**, 393 (2011).
10. T. Zimmermann, J. Rietdorf and R. Pepperkok, FEBS Lett. **546**, 87 (2003).
11. M.B. Sinclair, D. M. Haaland, J. A. Timlin and D. T. Jones, Appl. Opt. **45**, 6283 (2006)
12. C. J. R. Sheppard, and X. Q. Mao, J. Mod. Opt. **35** (7), 1169 (1988).
13. G. J. Brakenhoff, J. Squier, T. Norris, A. C. Biliton, M. H. Wade and B. Athey, J. Microsc. **181**, 253 (1996).
14. S. Kumazaki, M. Hasegawa, M. Ghoneim, Y. Shimizu, K. Okamoto, M. Nishiyama, H. Oh-oka and M. Terazima, J. Microsc. **228**, 240 (2007).
15. K. Hamada, K. Fujita, N. I. Smith, M. Kobayashi, Y. Inouye and S. Kawata, J. Biomed. Opt. **13**, 044027 (2008).
16. T. Matsuda, A. Miyawaki and T. Nagai, Nat. Methods **5**, 339 (2008).
17. H. W. Ai, J. N. Henderson, S. J. Remington and R. E. Campbell, Biochem. J. **400**, 531 (2006)
18. R. Y. Tsien, Annu. Rev. Biochem. **67**, 509 (1998.)
19. W. Tomosugi, T. Matsuda, T. Tani, T. Nemoto, I. Kotera, K. Saito, K. Horikawa and T. Nagai, Nat. Methods **6**, 351 (2009)
20. S. Kawata, R. Arimoto and O. Nakamura, J. Opt. Soc. Am. A **8**, 171 (1991).
21. E. Dusch, T. Dorval, N. Vincent, M. Wachsmuth and A. Genovesio, J. Microsc. **228**, 132 (2007).
22. T. Nagai, K. Ibata, E. S. Park, M. Kubota, K. Mikoshiba and A. Miyawaki, Nat. Biotechnol. **20**, 87 (2002).
23. M. V. Matz, A. F. Fradkov, Y. A. Labas, A. P. Savitsky, A. G. Zaraisky, M. L. Markelov and S. A. Lukyanov, Nat. Biothecnol. **17**, 969 (1999).
24. G. H. Patterson and D. W. Piston, Biophys. J. **78**, 2159 (2000).
25. A. Hopt, and E. Neher, Biophys. J. 80, 2029 (2001).
26. T.-S. Chen, S.-Q. Zeng, Q.-M. Luo, Z.-H. Zhang, and W. Zhou, Biochem. Biophys. Res. Commun. **291**, 1272 (2002).
27. S.-Y. Chen, C.-S. Lu, and C.-H. Yeh, Biomed. Opt. Express **5**, 338 (2014).
28. F. Deng, C. Ding, J. C. Martin, N. M. Scarborough, Z. Song, G. S. Eakins and G. J. Simpson Opt. Express **25**, 32243 (2017).
29. J. S. Marchant, G. E. Stutzmann, M. A. Leissring, F. M. LaFerla, and I. Parker, Nat. Biotechnol. **19**, 645 (2001).
30. J. Herz, V. Siffrin, A. E. Hauser, A. U. Brandt, T. Leuenberger, H. Radbruch, F. Zipp, and R. A. Niesner, Biophys. J. **98**, 715 (2010).
31. K. Otomo, T. Hibi, T. Murata, H. Watanabe, R. Kawakami, H. Nakayama, M. Hasebe and T. Nemoto, Analytical Sciences **31**, 307 (2015).
32. O. Mandula, M. Kielhorn, K. Wicker, G. Krampert, I. Kleppe and R. Heintzmann, Opt. Express **20,** 24167 (2012).
33. K. Watanabe, A. F. Palonpon, N. I. Smith, L-D Chiu, A. Kasai, H. Hashimoto, S. Kawata and K. Fujita, Nature Commun. **6**, 10095 (2015).
34. Y. J. Hsu, C.-C. Chen, C.-H. Huang, C.-H. Yeh, L.-Y. Liu, and S.-Y. Chen, Biomed. Opt. Express **8,** 3005 (2017).

## Full references


1. R. N. Day and M. W. Davidson, "The fluorescent protein palette: tools for cellular imaging," Chem. Soc. Rev. **38**, 2887–2921 (2009).
2. J. Lippincott-Schwartz and G. H. Patterson, "Development and use of fluorescent protein markers in living cells," Science **300**, 87–91 (2003).
3. J. Ellenberg, J. Lippincott-Schwartz, and J. F. Presley, "Dual-colour imaging with GFP variants," Trends Cell Biol. **9**, 52–56 (1999).
4. Q. Li, X. He, Y. Wang, H. Liu, D. Xu, and F. Guo, "Review of spectral imaging technology in biomedical engineering: achievements and challenges," J. Biomed. Opt. **18**, 100901 (2013).
5. M. Yamanaka, K. Saito, N. I. Smith, Y. Arai, K. Uegaki, Y. Yonemaru, K. Mochizuki, S. Kawata, T. Nagai, and K. Fujita, "Visible-wavelength two-photon excitation microscopy for fluorescent protein imaging," J. Biomed. Opt. **20**, 101202 (2015).
6. R. Oketani, H. Suda, K. Uegaki, T. Kubo, T. Matsuda, M. Yamanaka, Y. Arai, N. Smith, T. Nagai, and K. Fujita, "Visible-wavelength two-photon excitation microscopy with multifocus scanning for volumetric live-cell imaging," J. Biomed. Opt. **25**, 014502 (2019).
7. M. Drobizhev, F. Meng, A. Rebane, Y. Stepanenko, E. Nickel, and C. W. Spangler, "Strong two-photon absorption in new asymmetrically substituted porphyrins: interference between charge-transfer and intermediate-resonance pathways," J. Phys. Chem. B **110**, 9802–9814 (2006).
8. M. Drobizhev, N. S. Makarov, T. Hughes, and A. Rebane, "Resonance enhancement of two-photon absorption in fluorescent proteins," J. Phys. Chem. B **111**, 14051–14054 (2007).
9. M. Drobizhev, N. S. Makarov, S. E. Tillo, T. E. Hughes, and A. Rebane, "Two-photon absorption properties of fluorescent proteins," Nat. Methods **8**, 393–399 (2011).
10. T. Zimmermann, J. Rietdorf, and R. Pepperkok, "Spectral imaging and its applications in live cell microscopy," FEBS Lett. **546**, 87–92 (2003).
11. M. B. Sinclair, D. M. Haaland, J. A. Timlin, and H. D. T. Jones, "Hyperspectral confocal microscope," Appl. Opt. **45**, 6283–6291 (2006).
12. C. J. R. Sheppard and X. Q. Mao, "Confocal Microscopes with Slit Apertures," J. Mod. Opt. **35**, 1169–1185 (1988).
13. G. J. Brakenhoff, J. Squier, T. Norris, A. C. Bliton, M. H. Wade, and B. Athey, "Real-time two-photon confocal microscopy using a femtosecond, amplified Ti:sapphire system," J. Microsc. **181**, 253–259 (1996).
14. S. Kumazaki, M. Hasegawa, M. Ghoneim, Y. Shimizu, K. Okamoto, M. Nishiyama, H. Oh-Oka, and M. Terazima, "A line-scanning semi-confocal multi-photon fluorescence microscope with a simultaneous broadband spectral acquisition and its application to the study of the thylakoid membrane of a cyanobacterium Anabaena PCC7120," J. Microsc. **228**, 240–254 (2007).
15. K. Hamada, K. Fujita, N. I. Smith, M. Kobayashi, Y. Inouye, and S. Kawata, "Raman microscopy for dynamic molecular imaging of living cells," J. Biomed. Opt. **13**, 044027 (2008).
16. T. Matsuda, A. Miyawaki, and T. Nagai, "Direct measurement of protein dynamics inside cells using a rationally designed photoconvertible protein," Nat. Methods **5**, 339–345 (2008).
17. H.-W. Ai, J. N. Henderson, S. J. Remington, and R. E. Campbell, "Directed evolution of a monomeric, bright and photostable version of Clavularia cyan fluorescent protein: structural characterization and applications in fluorescence imaging," Biochem. J **400**, 531–540 (2006).
18. R. Y. Tsien, "The green fluorescent protein," Annu. Rev. Biochem. **67**, 509–544 (1998).
19. W. Tomosugi, T. Matsuda, T. Tani, T. Nemoto, I. Kotera, K. Saito, K. Horikawa, and T. Nagai, "An ultramarine fluorescent protein with increased photostability and pH insensitivity," Nat. Methods **6**, 351–353 (2009).
20. S. Kawata, R. Arimoto, and O. Nakamura, "Three-dimensional optical-transfer-function analysis for a laser-scan fluorescence microscope with an extended detector," J. Opt. Soc. Am. A, JOSAA **8**, 171–175 (1991).
21. E. Dusch, T. Dorval, N. Vincent, M. Wachsmuth, and A. Genovesio, "Three-dimensional point spread function model for line-scanning confocal microscope with high-aperture objective," J. Microsc. **228**, 132–138 (2007).
22. T. Nagai, K. Ibata, E. S. Park, M. Kubota, K. Mikoshiba, and A. Miyawaki, "A variant of yellow fluorescent protein with fast and efficient maturation for cell-biological applications," Nat. Biotechnol. **20**, 87–90 (2002).
23. M. V. Matz, A. F. Fradkov, Y. A. Labas, A. P. Savitsky, A. G. Zaraisky, M. L. Markelov, and S. A. Lukyanov, "Fluorescent proteins from nonbioluminescent Anthozoa species," Nat. Biotechnol. **17**, 969–973 (1999).
24. G. H. Patterson and D. W. Piston, "Photobleaching in two-photon excitation microscopy," Biophys. J. **78**, 2159–2162 (2000).
25. T.-S. Chen, S.-Q. Zeng, Q.-M. Luo, Z.-H. Zhang, and W. Zhou, "High-order photobleaching of green fluorescent protein inside live cells in two-photon excitation microscopy," Biochem. Biophys. Res. Commun. **291**, 1272–1275 (2002).
26. A. Hopt and E. Neher, "Highly nonlinear photodamage in two-photon fluorescence microscopy," Biophys. J. **80**, 2029–2036 (2001).
27. S.-Y. Chen, C.-S. Lu, and C.-H. Yeh, "Non-de-scanned parallel recording two-photon hyperspectral microscopy with high spectral and spatial resolution," Biomed. Opt. Express **5**, 338–347 (2014).
28. F. Deng, C. Ding, J. C. Martin, N. M. Scarborough, Z. Song, G. S. Eakins, and G. J. Simpson, "Spatial-spectral multiplexing for hyperspectral multiphoton fluorescence imaging," Opt. Express, OE **25**, 32243–32253 (2017).
29. J. S. Marchant, G. E. Stutzmann, M. A. Leissring, F. M. LaFerla, and I. Parker, "Multiphoton-evoked color change of DsRed as an optical highlighter for cellular and subcellular labeling," Nat. Biotechnol. **19**, 645–649 (2001).
30. J. Herz, V. Siffrin, A. E. Hauser, A. U. Brandt, T. Leuenberger, H. Radbruch, F. Zipp, and R. A. Niesner, "Expanding two-photon intravital microscopy to the infrared by means of optical parametric oscillator," Biophys. J. **98**, 715–723 (2010).
31. K. Otomo, T. Hibi, T. Murata, H. Watanabe, R. Kawakami, H. Nakayama, M. Hasebe, and T. Nemoto, "Multi-point scanning two-photon excitation microscopy by utilizing a high-peak-power 1042-nm laser," Anal. Sci. **31**, 307–313 (2015).
32. O. Mandula, M. Kielhorn, K. Wicker, G. Krampert, I. Kleppe, and R. Heintzmann, "Line scan--structured illumination microscopy super-resolution imaging in thick fluorescent samples," Opt. Express **20**, 24167–24174 (2012).
33. K. Watanabe, A. F. Palonpon, N. I. Smith, L. Chiu, A. Kasai, H. Hashimoto, S. Kawata, and K. Fujita, "Structured line illumination Raman microscopy," Nat. Commun. **6**, 10095 (2015).
34. Y. J. Hsu, C.-C. Chen, C.-H. Huang, C.-H. Yeh, L.-Y. Liu, and S.-Y. Chen, "Line-scanning hyperspectral imaging based on structured illumination optical sectioning," Biomed. Opt. Express **8**, 3005–3016 (2017).